

## Measurement Techniques

### INTRODUCTION

The characteristics of optoelectronics devices given in datasheets are verified either by 100 % production tests followed by statistic evaluation or by sample tests on typical specimens. These tests can be divided into following categories:

- Dark measurements
- Light measurements
- Measurements of switching characteristics, cut-off frequency and capacitance
- Angular distribution measurements
- Spectral distribution measurements
- Thermal measurements

Dark and light measurements limits are 100 % measurements. All other values are typical. The basic circuits used for these measurements are shown in the following sections. The circuits may be modified slightly to accommodate special measurement requirements.

Most of the test circuits may be simplified by use of a source measure unit (SMU), which allows either to source voltage and measure current or to source current and measure voltage.

### DARK AND LIGHT MEASUREMENTS

#### EMITTER DEVICES

##### IR Diodes (GaAs)

Forward voltage,  $V_F$ , is measured either on a curve tracer or statically using the circuit shown in figure 1. A specified forward current (from a constant current source) is passed through the device and the voltage developed across it is measured on a high-impedance voltmeter.

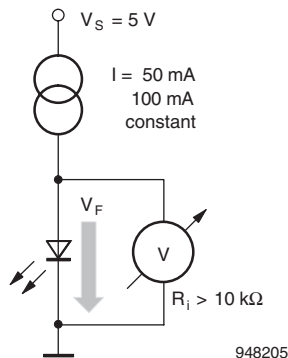


Fig. 1

To measure reverse voltage,  $V_R$ , a 10  $\mu$ A or 100  $\mu$ A reverse current from a constant current source is impressed through the diode (figure 2) and the voltage developed across it is measured on a voltmeter of high input impedance ( $\geq 10$  M $\Omega$ ).

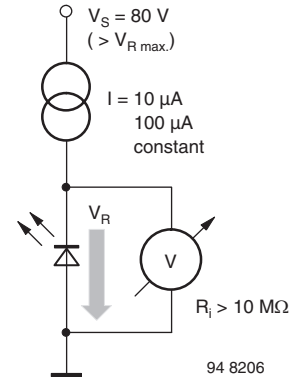


Fig. 2

For most devices,  $V_R$  is specified at 10  $\mu$ A reverse current. In this case either a high impedance voltmeter has to be used, or current consumption of DVM has to be calculated and added to the specified current. A second measurement step will then give correct readings.

In case of GaAs IR diodes, total radiant output power,  $\Phi_e$ , is usually measured. This is done with a calibrated large-area photovoltaic cell fitted in a conical reflector with a bore which accepts the test item - see figure 3. An alternative test set uses a silicon photodiode attached to an integrating sphere. A constant DC or pulsating forward current of specified magnitude is passed through the IR diode. The advantage of pulse-current measurements at room temperature (25  $^{\circ}$ C) is that results can be reproduced exactly.

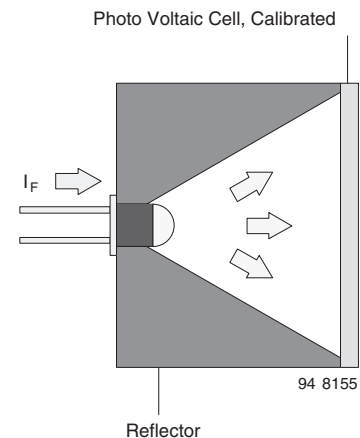


Fig. 3

If, for reasons of measurement economy, only DC measurements (figure 4) are to be made, then the energizing time should be kept short (below 1 s) and of uniform duration, to minimize any fall-off in light output due to internal heating.

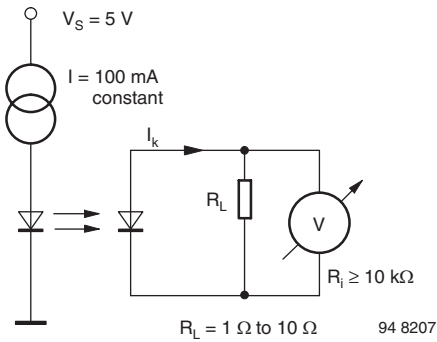


Fig. 4

To ensure that the relationship between irradiance and photocurrent is linear, the photodiode should operate near the short-circuit configuration. This can be achieved by using a low resistance load ( $\leq 10 \Omega$ ) of such a value that the voltage dropped across is very much lower than the open circuit voltage produced under identical illumination conditions ( $R_{meas} \ll R_i$ ). The voltage across the load should be measured with a sensitive DVM.

A knowledge of radiant intensity,  $I_e$ , produced by an IR emitter enables customers to assess the range of IR light barriers. The measurement procedure for this is more or less the same as the one used for measuring radiant power. The only difference is that in this case the photodiode is used without a reflector and is mounted at a specified distance from, and on the optical axis of, the IR diode (figure 5). This way, only the radiant power of a narrow axial beam is considered.

The radiant power within a solid angle of  $\Omega = 0.01$  steradian (sr) is measured at a distance of 100 mm. Radiant intensity is then obtained by using this measured value for calculating the radiant intensity for a solid angle of  $\Omega = 1$  sr.

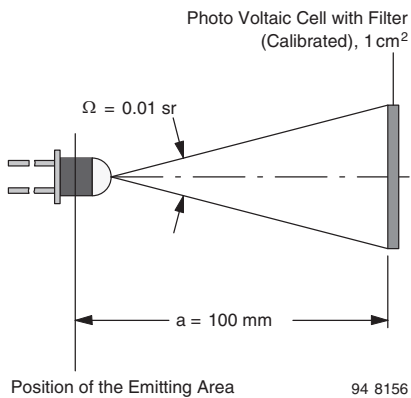


Fig. 5

## DETECTOR DEVICES

### Photovoltaic cells, photodiodes

- Dark measurements

The reverse voltage characteristic,  $V_R$ , is measured either on a curve tracer or statically using the circuit shown in figure 6. A high-impedance voltmeter, which draws only an insignificant fraction of device's reverse current, must be used.

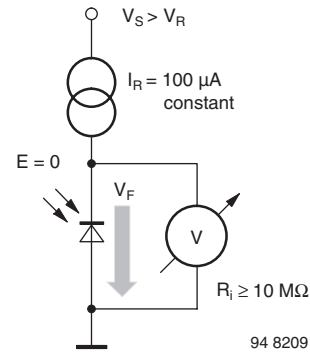


Fig. 6

Dark reverse current measurements,  $I_{ro}$ , must be carried out in complete darkness - reverse currents of silicon photodiodes are in the range of nanoamperes only, and an illumination of a few lx is quite sufficient to falsify the test result. If a highly sensitive DVM is to be used, then a current sampling resistor of such a value that voltage dropped across it is small in comparison with supply voltage must be connected in series with the test item (figure 7). Under these conditions, any reverse voltage variations of the test samples can be ignored. Shunt resistance (dark resistance) is determined by applying a very slight voltage to the photodiode and then measuring dark current. In case of 10 mV or less, forward and reverse polarity will result in similar readings.

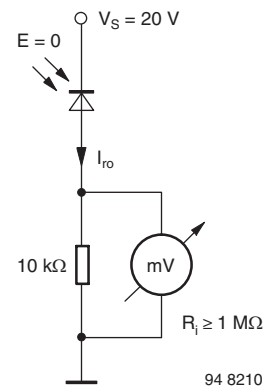


Fig. 7

- Light measurements

The same circuit as used in dark measurement can be used to carry out light reverse current,  $I_{ra}$ , measurements on photodiodes. The only difference is the diode is now irradiated and a current sampling resistor of lower value must be used (figure 8), because of the higher currents involved.

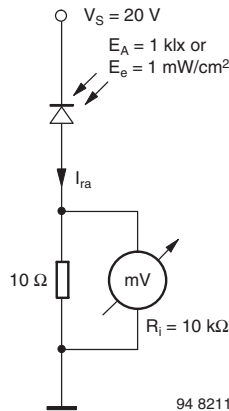


Fig. 8

The open circuit voltage,  $V_O$ , and short circuit current,  $I_k$ , of photovoltaic cells and photodiodes are measured by means of the test circuit shown in figure 9. The value of the load resistor used for the  $I_k$  measurement should be chosen so that the voltage dropped across it is low in comparison with the open circuit voltage produced under conditions of identical irradiation.

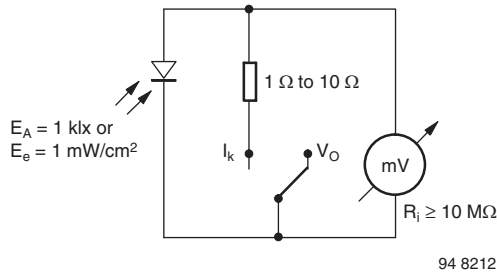


Fig. 9

The light source used for the light measurements is a calibrated incandescent tungsten lamp with no filters. The filament current is adjusted for a color temperature of 2856 K (standard illuminant A to DIN 5033 sheet 7). A specified illumination,  $E_v$ , (usually 100 lx or 1000 lx) is produced by adjusting the distance,  $a$ , between the lamp and a detector on an optical bench.  $E_v$  can be measured on a  $V(\lambda)$ -corrected luxmeter, or, if luminous intensity,  $I_v$ , of the lamp is known,  $E_v$  can be calculated using the formula:  $E_v = I_v/a^2$ .

It should be noted that this inverse square law is only strictly accurate for point light sources, that is for sources where the dimensions of the source (the filament) are small ( $\leq 10\%$ ) in comparison with the distance between the source and detector.

Since lux is a measure for visible light only, near-infrared radiation (800 nm to 1100 nm) where silicon detectors have their peak sensitivity is not taken into account. Unfortunately, the near-infrared emission of filament lamps of various construction varies widely. As a result, light current

measurements carried out with different lamps (but the same lux and color temperature calibration) may result in readings that differ up to 20 %.

The simplest way to overcome this problem is to calibrate (measure the light current) some items of a photodetector type with a standard lamp (OSRAM WI 41/G) and then use these devices for adjustment of the lamp used for field measurements.

An IR diode is used as a radiation source (instead of a Tungsten incandescent lamp), to measure detector devices being used mainly in IR transmission systems together with IR emitters (e.g., IR remote control, IR headphone). Operation is possible both with DC or pulsed current.

The adjustment of irradiance,  $E_e$ , is similar to the above mentioned adjustment of illuminance,  $E_v$ . To achieve a high stability similar to filament lamps, consideration should be given to the following two points:

- The IR emitter should be connected to a good heat sink to provide sufficient temperature stability.
- DC or pulse-current levels as well as pulse duration have great influence on self-heating of IR diodes and should be chosen carefully.
- The radiant intensity,  $I_e$ , of the device is permanently controlled by a calibrated detector.

**Phototransistors**

The collector emitter voltage,  $V_{CEO}$ , is measured either on a transistor curve tracer or statically using the circuit shown in figure 10. Normal bench illumination does not change the measured result.

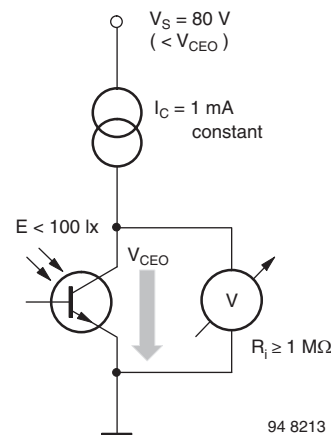


Fig. 10

In contrast, however, the collector dark current,  $I_{CEO}$  or  $I_{CO}$ , must be measured in complete darkness (figure 11). Even ordinary daylight illumination of the wire fed-through glass seals would falsify the measurement result.

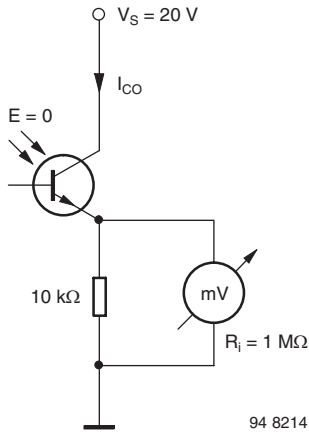


Fig. 11

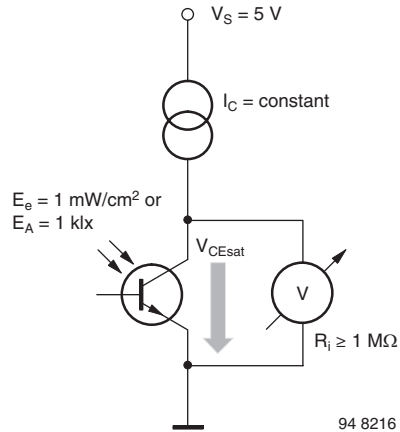


Fig. 13

The same circuit is used for collector light current,  $I_{ca}$ , measurements (figure 12). The optical axis of the device is aligned to an incandescent tungsten lamp with no filters, producing a CIE illuminance  $A$  of 100 lx or 1000 lx with a color temperature of  $T_f = 2856$  K. Alternatively an IR irradiance by a GaAs diode can be used (refer to the photovoltaic cells and photodiodes section). Note that a lower sampling resistor is used, in keeping with the higher current involved.

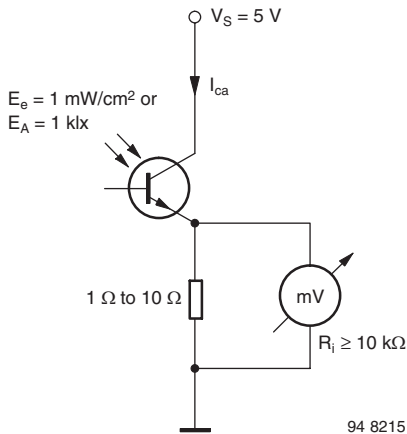


Fig. 12

To measure collector emitter saturation voltage,  $V_{CEsat}$ , the device is illuminated and a constant collector current is passed through. The magnitude of this current is adjusted below the level of the minimum light current,  $I_{ca min}$ , for the same illuminance (figure 13). The saturation voltage of the phototransistor (approximately 100 mV) is then measured on a high impedance voltmeter.

## SWITCHING CHARACTERISTICS

### Definition

Each electronic device generates a certain delay between input and output signals as well as a certain amount of amplitude distortion. A simplified circuit (figure 14) shows how input and output signals of optoelectronic devices can be displayed on a dual-trace oscilloscope.

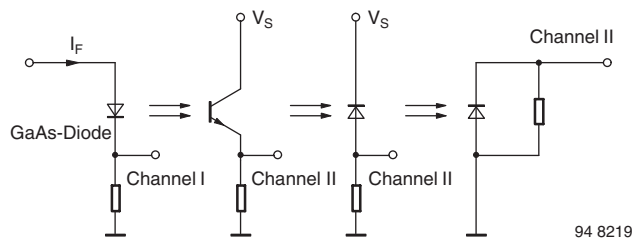


Fig. 14

The switching characteristics can be determined by comparing the timing of output current waveform with the input current waveform (figure 15).

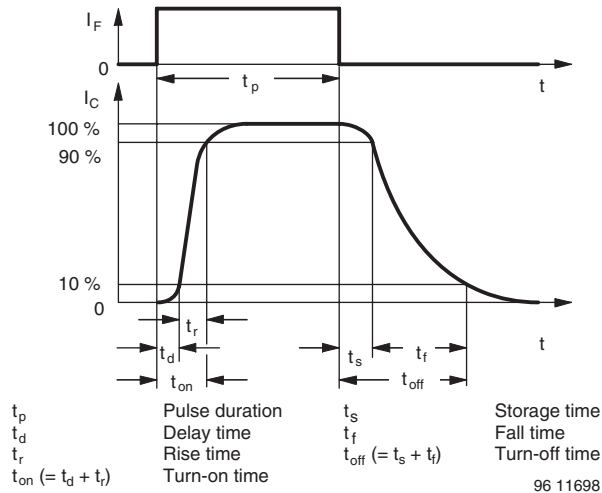


Fig. 15

These time parameters also include the delay existing in a luminescence diode between forward current ( $I_F$ ) and radiant power ( $\Phi_e$ ).

### Notes Concerning the Test Set-up

Circuits used for testing IR emitting, emitting sensitive and optically coupled isolator devices are basically the same (figure 14). The only difference is the way in which test device is connected to the circuit.

It is assumed that rise and fall times associated with the signal source (pulse generator) and dual trace oscilloscope are insignificant, and that the switching characteristics of any radiant sensitive device used in set-up are considerably shorter than those of the test item. The switching characteristics of IR emitters, for example ( $t_r \approx 10$  ns to 1000 ns), are measured with aid of a PIN Photodiode detector ( $t_r \approx 1$  ns).

Photo- and darlington transistors and photo- and solar cells ( $t_r \approx 0.5$   $\mu$ s to 50  $\mu$ s) are, as a rule, measured by use of fast IR diodes ( $t_r < 30$  ns) as emitters.

Red light-emitting diodes are used as light sources only for devices which cannot be measured with IR diodes because of their spectral sensitivity (e.g. BPW21R). These diodes emit only 1/10 of radiant power of IR diodes and consequently generate only very low signal levels.

### Switching Characteristic Improvements on Phototransistors and Darlington Phototransistors

As in any ordinary transistor, switching times are reduced if drive signal level, and hence collector current, is increased. Another time reduction (especially in fall time  $t_f$ ) can be achieved by use of a suitable base resistor, assuming there is an external base connection, although this can only be done at the expense of sensitivity.

## TECHNICAL DESCRIPTION - ASSEMBLY

### Emitter

Emitters are manufactured using the most modern liquid phase epitaxy (LPE) process. By using this technology, the number of undesirable flaws in the crystal is reduced. This results in a higher quantum efficiency and thus higher radiation power. Distortions in the crystal are prevented by using mesa technology which leads to lower degradation. A further advantage of the mesa technology is that each individual chip can be tested optically and electrically, even on the wafer.

### DETECTOR

Vishay Semiconductor detectors have been developed to match perfectly to emitters. They have low capacitance, high photosensitivity, and extremely low saturation voltage. Silicon nitride passivation protects surface against possible impurities.

### Assembly

Components are fitted onto lead frames by fully automatic equipment using conductive epoxy adhesive. Contacts are established automatically with digital pattern recognition using well-proven thermosonic techniques. All component are measured according to the parameter limits given in the datasheet.

### Applications

Silicon photodetectors are used in manifold applications, such as sensors for radiation from near UV over visible to near infrared. There are numerous applications in measurement of light, such as dosimetry in UV, photometry, and radiometry. A well known application is shutter control in cameras.

Another large application area for detector diodes, and especially phototransistors, is position sensing. Examples are differential diodes, optical sensors, and reflex sensors.

Other types of silicon detectors are built-in as parts of optocouplers.

One of the largest application areas is remote control of TV sets and other home entertainment appliances.

Different applications require specialized detectors and also special circuits to enable optimized functioning.

## Equivalent circuit

Photodiode diodes can be described by the electrical equivalent circuit shown in figure 16.

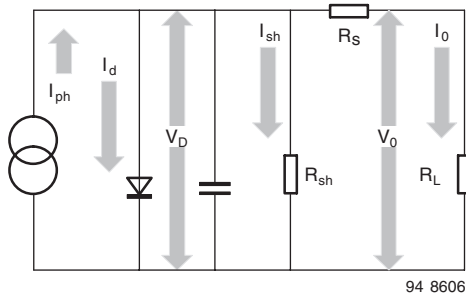


Fig. 16

$$I_O = I_{ph} - I_D - I_{sh} \quad (1)$$

$$I_O = I_{ph} - I_s \left( \exp \frac{qV_D}{kT} - 1 \right) - I_{sh}$$

$$V_{OC} = V_T \times \ln \left( \frac{s(\lambda) \times \phi_e - I_{sh}}{I_s} + 1 \right) \quad (2)$$

As described in the chapter “I-V Characteristics of illuminated pn junction”, the incident radiation generates a photocurrent loaded by a diode characteristic and load resistor,  $R_L$ . Other parts of the equivalent circuit (parallel capacitance,  $C$ , combined from junction,  $C_j$ , and stray capacitances, serial resistance,  $R_s$ , and shunt resistance,  $R_{sh}$ , representing an additional leakage) can be neglected in most standard applications, and are not expressed in equations 5 and 7 (see “Physics and Technology”). However, in applications with high frequencies or extreme irradiation levels, these parts must be regarded as limiting elements.

## Searching for the right detector diode type

The BPW 20 RF photodiode is based on rather highly doped n-silicon, while BPW34 is a PIN photodiode based on very lightly doped n-silicon. Both diodes have the same active area and spectral response as a function of wavelength is very similar. These diodes differ in their junction capacitance and shunt resistance. Both can influence the performance of an application.

Detecting very small signals is the domain of photodiodes with their very small dark currents and dark/shunt resistances.

With a specialized detector technology, these parameters are very well controlled in all Vishay photodetectors.

The very small leakage currents of photodiodes are offset by higher capacitances and smaller bandwidths in comparison to PIN photodiodes.

Photodiodes are often operated in photovoltaic mode, especially in light meters. This is depicted in figure 17, where

a strong logarithmic dependence of the open circuit voltage on the input signal is used.

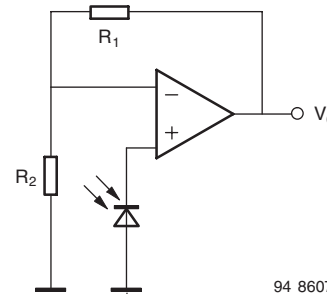


Fig. 17 - Photodiode in the Photovoltaic Mode Operating with a Voltage Amplifier

$$V_O \approx V_{OC} \times [1 + R_1/R_2] \quad \text{with} \quad (3)$$

$$V_{OC} = V_T \times \ln(s(\lambda) \times \phi_e / I_s + 1) \quad (2)$$

It should be noted that extremely high shunt/dark resistance (more than 15 GΩ) combined with a high-impedance operational amplifier input and a junction capacitance of about 1 nF can result in slow switch-off time constants of some seconds. Some instruments therefore have a reset button for shortening the diode before starting a measurement.

The photovoltaic mode of operation for precise measurements should be limited to the range of low ambient temperatures, or a temperature control of the diode (e.g., using a Peltier cooler) should be applied. At high temperatures, dark current is increased (see figure 18) leading to a non-logarithmic and temperature dependent output characteristic (see figure 19). The curves shown in figure 18 represent typical behavior of these diodes. Guaranteed leakage (dark reverse current) is specified with  $I_{r0} = 30$  nA for standard types. This value is far from that one which is typically measured. Tighter customer specifications are available on request. The curve shown in figure 19 show the open circuit voltage as a function of irradiance with dark reverse current,  $I_s$ , as a parameter (in a first approximation increasing  $I_s$  and  $I_{sh}$  have the same effect). The parameter shown covers the possible spread of dark current. In combination with figure 18 one can project the extreme dependence of the open circuit voltage at high temperatures (figure 20).

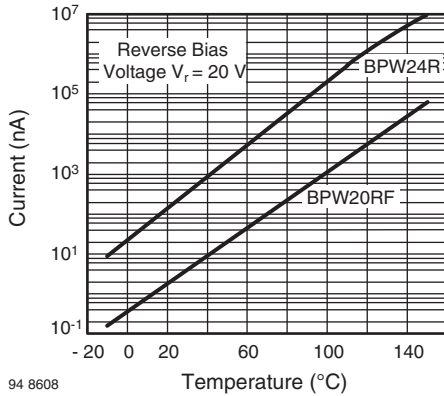


Fig. 18 - Reverse Dark Current vs. Temperature

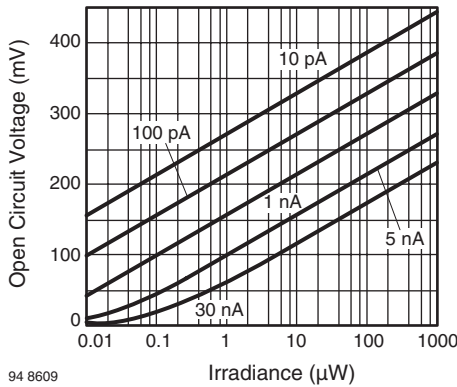


Fig. 19 - Open Circuit Voltage vs. Irradiance, Parameter: Dark Reverse Current, BPW20RF

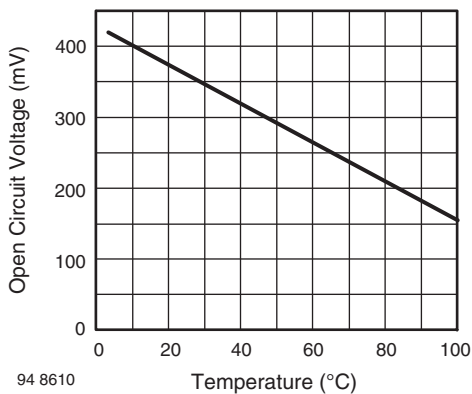


Fig. 20 - Open Circuit Voltage vs. Temperature, BPW46

### Operating modes and circuits

The advantages and disadvantages of operating a photodiode in open circuit mode have been discussed. For operation in short circuit mode (see figure 21) or photoconductive mode (see figure 22), current-to-voltage converters are typically used. In comparison with photovoltaic mode, the temperature dependence of the output signal is much lower. Generally, the temperature coefficient of the light reverse current is positive for irradiation with wavelengths > 900 nm, rising with increasing wavelength. For wavelengths < 600 nm, a negative temperature coefficient is found, likewise with increasing absolute value to shorter wavelengths. Between these wavelength boundaries the output is almost independent of temperature. By using this mode of operation, the reverse biased or unbiased (short circuit conditions), output voltage,  $V_O$ , will be directly proportional to incident radiation,  $\phi_e$  (see equation in figure 21).

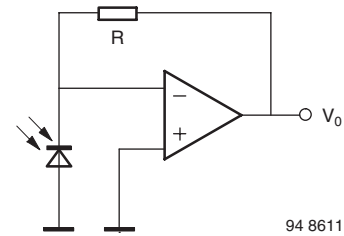


Fig. 21 - Transimpedance Amplifier, Current to Voltage Converter, Short Circuit Mode

$$V_O = -R \times \Phi_e \times s(\lambda) \tag{4}$$

$$V_O = -I_{sc} \times R \tag{5}$$

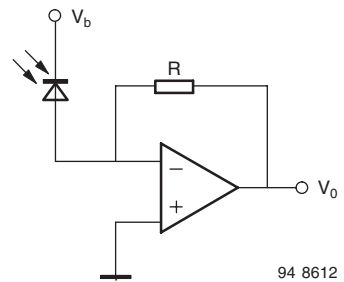


Fig. 22 - Transimpedance Amplifier, Current to Voltage Converter, Reverse Biased Photodiode

The circuit in figure 21 minimizes the effect of reverse dark current while the circuit in figure 22 improves the speed of the detector diode due to a wider space charge region with decreased junction capacitance and field increased velocity of the charge carrier transport.



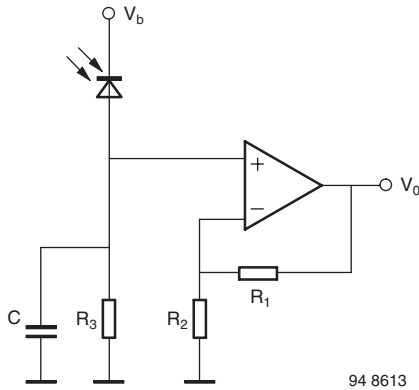


Fig. 23 - RC-Loaded Photodiode with Voltage Amplifier

Figure 23 shows photocurrent flowing into an RC load, where C represents junction and stray capacity while R<sub>3</sub> can be a real or complex load, such as a resonant circuit for the operating frequency.

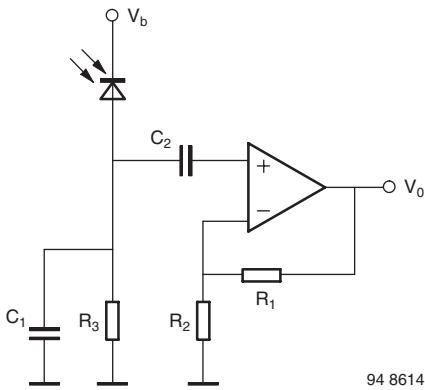


Fig. 24 - AC-Coupled Amplifier Circuit

$$V_O \approx \phi_e \times s(\lambda) \times R_3 \times [1 + R_1/R_2] \quad (6)$$

The circuit in figure 24 is equivalent to figure 23 with a change to AC coupling. In this case, the influence of background illumination can be separated from a modulated signal. The relation between input signal (irradiation,  $\phi_e$ ) and output voltage is given by the equation in figure 24.

### Frequency response

The limitations of switching times in photodiodes are determined by carrier lifetime. Due to the absorption properties of silicon, especially in photodiodes, most of incident radiation at longer wavelengths is absorbed outside the space charge region. Therefore, a strong wavelength dependence of the switching times can be observed (figure 25).

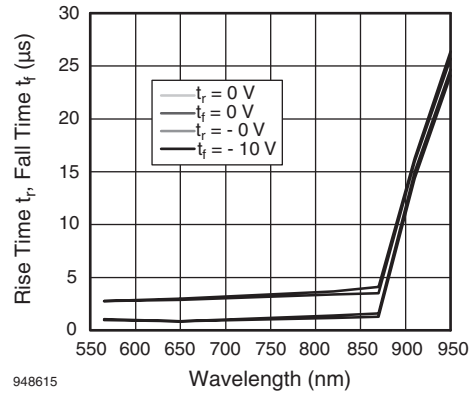


Fig. 25 - Switching Times vs. Wavelength for Photodiode BPW20RF

A drastic increase in rise and fall times is observed at wavelengths > 850 nm. Differences between unbiased and biased operation result from the widening of the space charge region.

However, for PIN photodiodes (BPW34/TEMD5000 family) similar results with shifted time scales are found. An example of such behavior, in this case in the frequency domain, is presented in figure 26 for a wavelength of 820 nm and figure 27 for 950 nm.

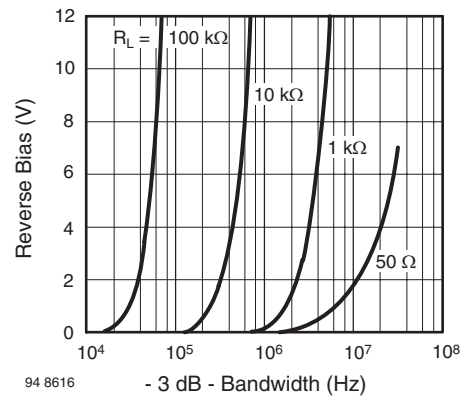


Fig. 26 - BPW34, TEMD5010X01, Bandwidth vs. Reverse Bias Voltage, Parameter: Load Resistance,  $\lambda = 820$  nm



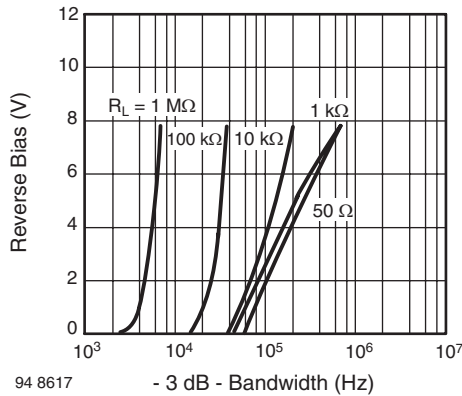


Fig. 27 - BPW41, TEMD5110X01, Bandwidth vs. Reverse Bias Voltage, Parameter: Load Resistance  $\lambda = 950$  nm

Below about 870 nm, only slight wavelength dependence can be recognized, while a steep change of cut-off frequency takes place from 870 nm to 950 nm (different time scales in figure 26 and figure 27). Additionally, the influence of load resistances and reverse bias voltages can be taken from these diagrams.

For cut-off frequencies greater than 10 MHz to 20 MHz, depending on the supply voltage available for biasing the detector diode, PIN photodiodes are also used. However, for this frequency range, and especially when operating with low bias voltages, thin epitaxially grown intrinsic (i) layers are incorporated into PIN photodiodes.

As a result, these diodes (e.g., Vishay's TESP5700) can operate with low bias voltages (3 V to 4 V) with cut-off frequencies of 300 MHz at a wavelength of 790 nm. With application-specific optimized designs, PIN photodiodes with cut-off frequencies up to 1 GHz at only a 3 V bias voltage with only an insignificant loss of responsivity can be generated. The main applications for these photodiodes are found in optical local area networks operating in the first optical window at wavelengths of 770 nm to 880 nm.

### WHICH TYPE FOR WHICH APPLICATION?

In table 1, selected diode types are assigned to different applications. For more precise selection according to chip sizes and packages, refer to the tables in introductory pages of this data book.

TABLE 1 - PHOTODIODE REFERENCE TABLE			
DETECTOR APPLICATION	PIN PHOTODIODE	PHOTODIODE	EPI PIN PHOTODIODE
Photometry, light meter		BPW21R	
Radiometry	TEMD5010X01, BPW34, BPW24R, ...	BPW20RF	
Light barriers	BPV10NF, BPW24R		
Remote control, IR filter included, $\lambda > 900$ nm	BPV20F, BPV23F, BPW41N, S186P, TEMD5100X01		
IR Data Transmission $f_c < 10$ MHz IR filter included, $\lambda > 820$ nm	BPV23NF, BPW82, BPW83, BPV10NF, TEMD1020, TEMD5110X01		
IR Data Transmission, $f_c > 10$ MHz, no IR filter	BPW34, BPW46, BPV10, TEMD5010X01		TESP5700
Densitometry	BPW34, BPV10, TEMD5010X01	BPW20RF, BPW21R	
Smoke detector	BPV22NF, BPW34, TEMD5010X01		

### PHOTOTRANSISTOR CIRCUITS

A phototransistor typically operates in a circuit shown in figure 28. Resistor  $R_B$  can be omitted in most applications. In some phototransistors, the base terminal is not connected.  $R_B$  can be used to suppress background radiation by setting a threshold level (see equation 7 and 8)

$$V_O = V_S - B \times \phi_e \times s(\lambda) \times R_L \quad (7)$$

$$V_O \approx V_S - (B \times \phi_e \times s(\lambda) - 0.6/R_B) \times R_L \quad (8)$$

For the dependence of rise and fall times on load resistance and collector-base capacitance, see the chapter "Properties of Silicon Phototransistors".

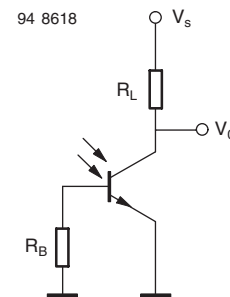


Fig. 28 - Phototransistor with Load Resistor and Optional Base Resistor